

Attosecond betatron radiation pulse train

V. Horný^{1,2,3}, M. Krůš², W. Yan⁴, T. Fülöp¹

¹ Department of Physics, Chalmers University of Technology, Gothenburg, Sweden

² Institute of Plasma Physics, Czech Academy of Sciences, Prague, Czechia

³ Laboratoire pour l'Utilisation des Lasers Intenses, Palaiseau, France

⁴ ELI Beamlines, Dolní Břežany, Czechia

Betatron radiation produced in the interaction of high-intensity laser with an underdense target [1] can already be considered as an established source of hard X-rays. Its main advantages are the source size in the order of microns and the high level of collimation along the laser axis [2]. The radiation emission accompanies the process of the laser wakefield acceleration of electrons. The electrons trapped in the electrostatic wake wave dragged by an relativistic laser pulse through a mm- to cm-scale plasma layer experience, in addition to the longitudinal acceleration, also a transverse motion caused by the transverse fields of the wakefield. These transverse betatron oscillations lead to emission of electromagnetic radiation. As electrons are highly relativistic, the critical energy of the synchrotron-like energy is in the X-ray range.

Typically, the electron bunch duration is several femtoseconds [3]. Generally, the electron spatial distribution within the captured bunch is set mainly by the injection process. The longitudinal electron bunch density profile remains continuous during the whole acceleration process, even though its exact shape develops during the acceleration stage as the electrons located at different longitudinal positions within the bunch experience different acceleration force as the wakefield is typically stronger at the rear part of the bubble, however, the effect of beam-loading effect might compensate it to a certain extent. The features of the betatron radiation can be understood as a fingerprint of the spatial and energy distribution of the electrons the electron bunch is comprised of. Therefore a standard betatron radiation is a continuous X-ray pulse and its duration is practically same as the as the electron bunch length.

Our earlier work showed that a train of ultrashort X-ray pulses can be produced by modifying the standard laser wakefield accelerator setup producing the betatron radiation. This can be accomplished by an additional laser field co-propagating behind the plasma wave drive pulse

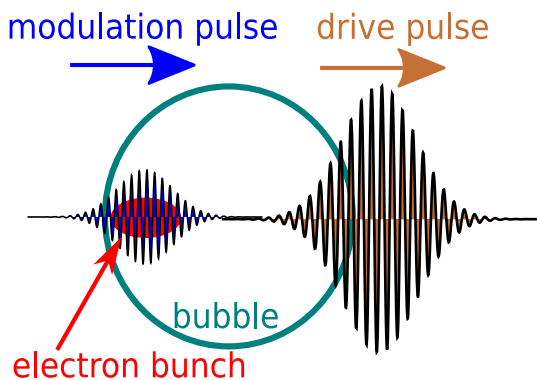


Figure 1: Modulation laser pulse transforms the electron bunch into the bunch train [4].

delayed by distance slightly less than the plasma wavelength. This laser field can modulate the electron bunch into two trains of electron bunches [4]. The trains are located in the laser polarisation plane, below and above the laser axis, respectively. The scheme of the configuration is shown in Figure 1.

Here, we offer additional illustrations to aid the understanding of the process presented in [4]. For the purpose of this conference contribution, the simulations by the 2D version of the EPOCH PIC code [5] were re-run with finer resolution than what was presented in Ref. [4]. The simulation box size was $80 \mu\text{m} \times 40 \mu\text{m}$. The grid resolution was 120 and 24 cells per drive pulse wavelength λ_d in the longitudinal and transverse directions, respectively. Initially, four electron macroparticles were placed in every cell. The plasma is represented as an electron gas; the ions were considered as a homogeneous static background.

The parameters used in the simulation are the following: plasma electron density $n_0 = 2.5 \times 10^{18} \text{ cm}^{-3}$, driver laser wavelength $\lambda_d = 0.8 \mu\text{m}$, waist size (radius at $1/e^2$ of maximum intensity) $w_0 = 10 \mu\text{m}$, pulse length (FWHM of intensity) $\tau = 20 \text{ fs}$, and normalized driver laser intensity $a_{0,d} = eE_{0,d}/m_e c \omega_0 = 1.8$ which corresponds to intensity $I = 6.9 \times 10^{18} \text{ W cm}^{-2}$. Its focal spot is located at $x_{f,m} = 110 \mu\text{m}$. The modulation pulse has the same fundamental parameters with the exception of normalized intensity, which is $a_{0,m} = 0.2$, and wavelength $\lambda_m = \lambda_d/3$ corresponding to intensity $7.7 \times 10^{17} \text{ W cm}^{-2}$. It is delayed by 58 fs and its focal spot is located at $x_{f,m} = 410 \mu\text{m}$. Both pulses are linearly polarized in the y -direction.

The delay between the respective bunches within the train is the wavelength of the modulation pulse λ_m . Both trains are shifted to each other by a distance $\lambda_m/2$. The neighbouring bunches of both trains are connected by a wire comprised of electrons of a lower density. The whole snake-like structure is plotted in the shades of grey in the upper panel of Figure 2, and the blue to red diverging colormap shows that the modulation pulse field dominates over the electrostatic wakefield. The respective micro-bunches of the trains are not comprised of the same electrons for the whole time. Each single electron travels in the direction backwards with respect to the snake-like structure, as it can be seen from the trajectories in Figure 2.

The left bottom panel shows how the amplitude of the transverse oscillation grows as the electrostatic wakefield which sustains the electrons within the bubble weakens during the laser propagation through the plasma. The other two panels capture the oscillations of the longitudinal and transverse velocity of the selected electrons, respectively. The longitudinal velocity of the electrons is the highest at the time when their transverse velocity is equal to zero, due to relativistic limitations. Therefore, the microbunches, i.e. the regions of an increased electron density, are generated there. At the same time, electrons radiate the most at the peaks of

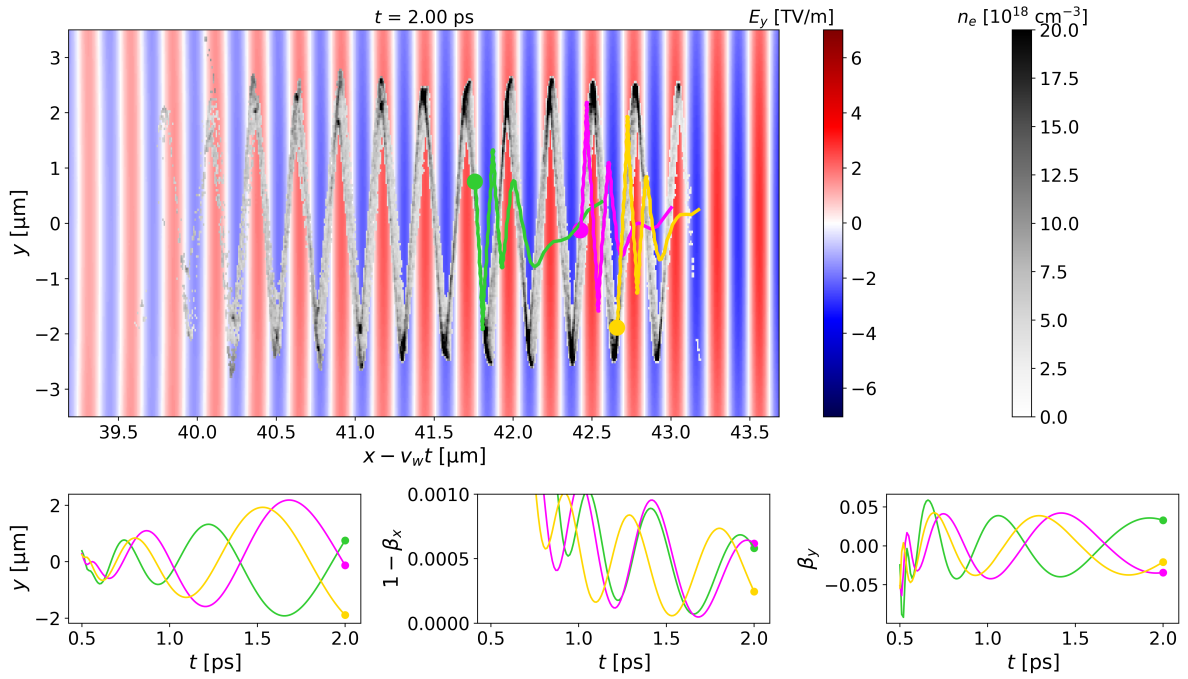


Figure 2: PIC simulations of the modulated betatron motion. Upper panel - transverse electric field is dominated by the modulation pulse (blue to red colormap); electron micro-bunches and the snake-like structure (grey colormap); trajectory of three randomly selected electrons. Bottom panel - transverse position (left), relative difference of the longitudinal velocity to the speed of light in vacuum (middle), and the relative transverse velocity (right) for the same randomly selected electrons.

their sine-like trajectory, since their acceleration is the largest there. Consequently, the whole snake-like structure can be understood as a device comprised of the equidistant emitters which continuously radiate the electromagnetic signal in the same direction as it propagates with the velocity close to the speed of light in vacuum. Practically, the radiated photons and radiating electrons co-propagate. The observer sitting at the far field at the laser propagation axis eventually receives a signal comprised of a series of flashes separated by $\lambda_m/2c$.

If the third harmonic of a standard Ti:sapphire laser pulse is considered ($\lambda_m = 267$ nm), the corresponding interval between the flashes is 444 as and the length of the single flash is around 100 as. Also, as it is shown in Figure 3, the temporal profile of the synchrotron radiation critical energy is modulated by the factor of $\lambda_m/2c$. It also shows how the critical energy of the

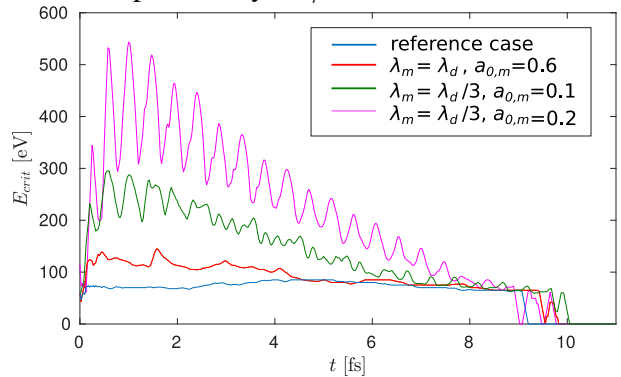


Figure 3: Modulation of the betatron pulse critical energy profile for several modulation pulse parameters.

radiation is generally greater when the modulation pulse is present and that it increases as λ_m decreases and $a_{0,m}$ grows.

In summary, through this scheme the standard betatron radiation from plasma wakefield accelerators can be converted to a train of sub-femtosecond X-ray pulses relatively easily. The distance between the single pulses of a train can be controlled by choosing the wavelength of the modulation laser pulse. Such a high-intensity X-ray source has a great potential to capture the dynamics of ultrafast processes and therefore has a wide range of applications in many fields of science. It can be used to improve the resolution of diagnostic techniques based on ultrashort hard X-rays [6] by an order of magnitude, whilst maintaining its other advantageous features such as a small source size of several microns enabling high-resolution images and a relatively small cost of the required laser systems compared to the large scale facilities such as synchrotrons or free electron lasers. It can also be used for laboratory astrophysics applications, for example to study warm dense matter with X-ray absorption spectroscopy. Broadband synchrotron X-ray pulses can be used also in solid state physics for polychromatic (Laue) X-ray diffraction, where the different energies are diffracted in different angles. Such technique can be used for determining the lattice structure of solid materials and the vibrations of its lattice.

Acknowledgments This work was supported by funding from the European Research Council (ERC) under the European Union's Horizon 2020 research and innovation program (Grant Agreements No. 787539 and No. 647121). The project has also received funding from the Knut och Alice Wallenberg Foundation. Simulations were performed on the Irene-Joliot-Curie machine hosted at TGCC, France, using High Performance Computing resources from GENCI-TGCC (Grant No. 2020-x2016057678).

References

- [1] S. Kiselev, A. Pukhov and I. Kostyukov, *Physical Review Letters* **93**, 135004 (2004).
- [2] S. Corde *et al.*, *Reviews of Modern Physics* **85**, 1 (2013).
- [3] E. Esarey C. B. Schroeder, and W. P. Leemans, *Reviews of Modern Physics* **81.3**, 1229, (2009).
- [4] V. Horný, M. Krůš, W. Yan and T. Fülöp, *Scientific Reports* **10.1**, 1-8 (2020).
- [5] T. D. Arber *et al.* *Plasma Physics and Controlled Fusion* **57.11**, 113001 (2015).
- [6] M. M. Martin and J. T. Hynes, *Femtochemistry and Femtobiology: Ultrafast Events in Molecular Science* Elsevier, Oxford (2004).